POSGRADO INTERINSTITUCIONAL EN CIENCIA Y TECNOLOGÍA

CENTRO DE INVESTIGACIONES EN ÓPTICA A.C.

INSPECTION OF PARABOLIC TROUGH COLLECTORS USING DIGITAL IMAGE PROCESSING

THESIS

TO OBTAIN THE ACADEMIC DEGREE OF:

MASTRO EN CIENCIA Y TECNOLOGÍA EN MECATRÓNICA

PRESENTS:

Alan Brian Diaz Reyna

DIRECTOR: **Dr. Luis Manuel Valentín Coronado**
CO-DIRECTOR: **Dr. Manuel I. Peña Cruz**

AGUASCALIENTES, AGS.
OCTOBER 15, 2024

Acknowledgements

To my Family.
"First of all, I would like to thank my mother, Graciela Reyna Lopez, my wife, Alejandra Muñoz Gutierrez, and my sister, Casandra Diaz Reyna, who have always given me their unconditional support to be able to achieve all my personal and academic goals. They are the ones who, with their love, have always encouraged me to pursue my goals and never abandon them in the face of adversity. They are also the ones who have given me the material and economic support to be able to concentrate on my studies and never abandon them".

To my tutor, Ph.D. Luis Manuel Valentin Coronado.
"I am deeply grateful to my tutor for his dedication and patience, without his precise words and corrections I would not have been able to reach this long-awaited instance. Thank you for his guidance and all his advice, I will carry them forever in my memory in my professional future".

To all my teachers.
"There are many teachers who have been part of my university path, and I want to thank all of them for transmitting the necessary knowledge to be able to be here today. Without you, the concepts would be just words, and we already know who takes the words, the wind.

To the CIO.
"Lastly, I would like to thank the CIO who has demanded so much of me but, at the same time, has allowed me to obtain my long-awaited

degree. I thank each manager for their work and for managing it, without which there would be no bases or conditions to learn knowledge.

Contents

List of figures

List of tables

Glossary

AI	Artificial Intelligence
CNN	Convolutional Neural Network
CSP	Concentrating Solar Power
DL	Deep Learning
DNI	Direct Normal Irradiance
FN	False Negatives
FP	False Positives
GHI	Global Horizontal Irradiance
GUI	Graphical User Interface
IoU	Intersection over Union
PTC	Parabolic-Trough Collector
PV	Photovoltaic
ROI	Region of Interest
TP	True Positives
UAV	Unmanned Aerial Vehicle

1

Introduction

An essential alternative to reducing gas emissions primarily caused by fossil fuels is the use of renewable energies. Applications such as heat generation, refrigeration, and electric power generation have started to be implemented using these clean energy sources. Among the various renewable sources, solar energy is the most abundant and is available anywhere on Earth. Consequently, many countries, including Mexico, are actively promoting research and technological development in the field of solar energy. One of the most advanced technologies in utilizing solar energy is the parabolic trough collector (PTC). PTCs capture solar radiation and convert it into heat, which is then transferred to a working fluid. Because these collectors rely on solar energy, they must be installed outdoors, making them more susceptible to dirt accumulation, which can reduce their efficiency.

Currently, visual inspections are carried out by individuals to determine if cleaning is necessary. This method is impractical as it relies on subjective judgment and personal experience, leading to inconsistent assessment criteria. To address this issue, a proposed solution is to develop a system capable of autonomously detecting different levels of dust deposition on the receiver tube of parabolic trough collectors. This system would analyze images taken by a camera mounted on an unmanned aerial vehicle (UAV) using a deep-learning approach. Figure 1.1 illustrates the proposed system. To address the challenge of localizing the collectors in the parabolic trough, a semantic segmentation neural network is proposed. This approach resolves the issue of developing an automatic system

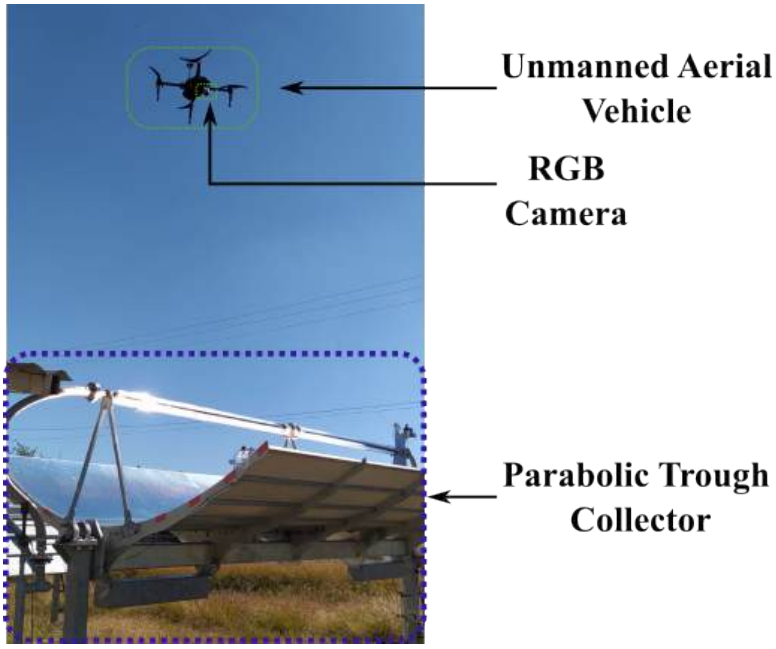

Figure 1.1: Unmanned Aircraft Vehicle taken images from a parabolic trough collector.

capable of detecting the collector and analyzing it to determine its level of dust. Once this is accomplished, a graphical interface will be developed, resulting in user-friendly software for final implementation and use.

1.1 Background

Parabolic trough collectors are a widely used technology in concentrating solar power (CSP) systems to harness solar energy efficiently. These systems use mirrors to focus sunlight onto a receiver tube, heating a fluid that generates steam to drive turbines for electricity production. However, one of the critical challenges that impact the efficiency of PTCs is dust deposition on the reflective surfaces of the mirrors and the glass covering the receiver tube. Dust particles reduce the reflectivity of the mirrors and decrease the amount of solar radiation that reaches the receiver, leading to a significant drop in thermal efficiency. This problem is especially prevalent in arid regions, where CSP plants are often located, and dust accumulation can be rapid. The decreased efficiency not only increases opera-

tional costs, as frequent cleaning is required, but also reduces the overall energy output, undermining the potential benefits of solar energy as a clean and sustainable energy source. Addressing dust deposition is crucial for optimizing the performance and cost-effectiveness of PTC-based solar power plants.

1.2 Problem definition

Dust accumulation on the surface of a solar collector reduces the amount of solar radiation that reaches the conversion device by decreasing the transmittance of the protective cover of non-concentrating collectors . Consequently, the impact of dust accumulation on the efficiency of solar photovoltaic (PV) modules and protective transparent covers has been extensively studied.

Erdenedavaa et al. (2018) investigated the effects of dust accumulation on the transmittance of glass tubes in a solar thermal collector in Usamentiaga et al. (2020). Effective solar radiation transmittance prediction models on transparent covers have been developed to evaluate the optimal cleaning time.

Zefri et al. (2018) developed a model to calculate the optimum tilt angle for soiled PV systems, considering dust accumulation rather than just irradiance. Additionally, Salari and Hakkaki-Fard (2019) numerically examined the impact of dust accumulation on the performance of PV and photovoltaic-thermal systems. Zhao and Zhang (2020) investigated dust deposition processes and behavior on ground-mounted solar PV arrays using the shear stress transport turbulence model and the discrete particle model.

These studies focused on the effect of dust accumulation on optical transmittance loss. For conventional non-concentrating panels, the direct and indirect light scattered from dust particles on the glass package can still reach the solar cell. However, an optical concentrating system collects sunlight more efficiently. When the surface of the dust collector is contaminated, a significant portion of the light is scattered and lost. Therefore, it is crucial to study concentrator loss. The research methods investigating the effects of dust accumulation on optical performance and the development of dust deposition models, as well as numerical investigations, provide valuable guidance for studying the impact of dust on the optical properties of reflectors.

These findings highlight the significant effects of dust accumulation on solar PV systems. Light interactions with dust particles can lead to even greater losses on reflective surfaces. Therefore, understanding the mechanisms of dust deposition is crucial for developing optimized cleaning strategies for reflectors. Cohen et al. (1999) proposed that dust accumulation on solar reflectors reduces their reflectivity by absorbing and scattering sunlight, with cleaning initiated when reflectivity drops below 90%. Pettit and Freese (1980) investigated the reflectivity loss on mirrors due to dust deposition over a 10-month period, finding that the average decrease in reflectivity at 500 nm was slightly less for silvered glass mirrors compared to aluminized reflective mirrors (Bagavathiappan et al., 2013).

The efficiency of cleaning operations depends on the cleaning frequency and the properties of the dust adhering to the solar reflector surface. Research into the characteristics of dust and soil at various sites is essential to understand the stickiness between dust and mirrors. Azouzoute et al. (2020) developed a mirror sphere with three tilt angles relative to the vertical plane: 45° (facing the sky), 0° (vertical), and −45° (facing the ground). Their results showed that the highest average cleanliness drop values per month were 45% for horizontal mirrors and 33% for vertical mirrors.

Vivar et al. (2010) used artificial dust on plane mirrors to test reflectivity, finding an average reflectivity loss of 20% compared to clean mirrors. The maximum daily reflectivity loss was 0.7–1.3% per day. Hachicha et al. (2019) studied the characteristics of dust particles and their impact on CSP performance under UAE weather conditions, reporting a reflectivity decrease of about 63% after three months of exposure.

Recent studies have reported various modeling methods to predict the decrease in reflectivity of dusty mirrors. Bouaddi et al. (2015) developed a model to describe and forecast the loss of reflectivity on solar reflectors used in CSP plants, using time series analysis with dynamic linear Gaussian state space models and incorporating weather parameters as explanatory variables. They also proposed a new approach to simulate the soiling of regularly cleaned reflectors, addressing the inaccuracies of fixed reflectivity assumptions in CSP yield estimations (Cipriani et al., 2020).

Biryukov et al. (1999) created a computerized microscopic system to study the physics of dust particles adhering to different solar collector surfaces. This system provided particle size distribution data, which helped calculate the fraction of the surface area covered by dust and the resulting reduction in optical efficiency based on particle size.

Heimsath and Nitz (2019) presented a model predicting mirror reflectivity for various cleanliness levels, applying the Lambert-Beer law to relate incidence angle-dependent attenuation of solar radiation to the dust layer. Another novel model measured airborne dust concentration, estimated the size distribution, and considered the position of the mirrors, wind speed, and air temperature.

Despite these advances, few studies have specifically examined the effect of dust accumulation on reflectivity at different positions on the surface of a reflector in a parabolic trough solar concentrator.

1.3 Justification

The parabolic-trough collectors are a great source of electricity and heat. It is estimated that, in a typical factory, the heat demand in the process can range from 40% to 60% of the total energy consumed and that 30% of that heat is used on temperatures of $80°C$ to $250°C$, so it is a good option for the development of the country.

Additionally, it is indispensable that PTCs have an appropriate performance, hence the importance of counting with mechanisms that ensure its optimum functioning through the detection of dirty.

Therefore, this project aims to develop an integrated vision system and a neural network capable of detecting dirt in parabolic trough collectors.

1.4 Objectives

1.4.1 General objective

Create a graphical interface where the end user can interact in a friendly way and thus recognize the presence of dirt in the parabolic trough PTCs and thus

promote their correct operation in the best performance. In this way, to improve the development of new technologies that are friendly to the environment, such as these systems.

1.4.2 Specifics objectives

- Develop a Convolutional Neural Network.
- Develop a Semantic Segmentation for tube detection.
- Create an Embedded interface.

1.5 Hypothesis

A vision system integrated into a neural network will be able to detect the dirt in a parabolic-trough collector, thereby increasing its performance.

2

Theoretical Framework

The improvement in quality of life and high demographic growth globally has led to a direct increase in energy demand. Therefore, it is crucial to develop strategies to meet these growing needs, especially considering that common energy resources such as oil, coal, natural gas, and uranium are becoming increasingly scarce. As demand approaches the limits of our ability to refine and extract these resources, prices continue to rise. The finite nature of these fuels has compelled us to seek greater efficiency in energy production and use, as well as to advance science and technology to enable renewable energies to compete with the generation costs of fossil fuels.

Renewable Energies are those that convert natural phenomena such as solar radiation, wind, waterfalls, to name a few, into forms of energy such as electricity and thermal energy. Renewable energies have great potential. However, most of them face two great challenges; intermittency and variability. However, despite these challenges, renewable energies have proven to be cost-effective compared to fossil fuels.

Mexico is geographically situated between 14° and 33° Latitude, a prime location for solar energy utilization. The national average daily global irradiation is approximately $5.5\,\mathrm{kWh/m^2}$ day, making Mexico one of the countries with the highest potential for solar energy generation worldwide (Pérez-Denicia et al., 2017). This potential is especially pronounced in the northern and central regions, which receive some of the highest levels of solar radiation globally. This abundant solar resource can be effectively harnessed for concentrated solar power

(CSP) technologies, such as parabolic trough collectors (PTCs), providing a significant opportunity for clean energy development. Figure 2.1 shows the distribution of DNI and GH irradiance in Mexico.

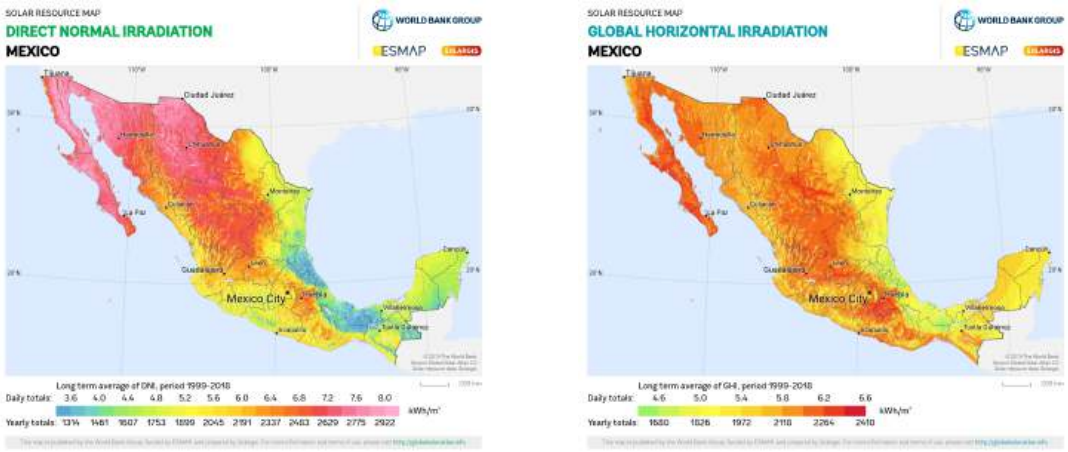

(a) **(b)**

Figure 2.1: Solar irradiance in Mexico. (a) DNI irradiance. (b) GHI irradiance

2.1 Parabolic-Trough Collectors

Photothermal solar collectors convert solar energy into thermal energy. These systems transfer energy from a distant radiant source (the Sun) to a fluid. Without the use of optical concentration, the maximum flux of incident solar energy radiation $1000W/m^2$ approximately (Moghimi and Ahmadi, 2018). With these radiative flux levels, solar flat plate collectors can be designed for applications where fluid temperatures need to be up to 100°C. However, many other applications require temperatures higher than those typically achieved by flat plate collectors. These higher temperatures can be achieved by placing an optical device between the sun and the energy-absorbing surface to increase the density of the incident radiative flux on the absorber. Such systems, which include both the optical device and the absorber, are referred to as solar collectors (LACYQS Laboratorio Nacional de Sistemas de Concentracion y Quimica Solar, 2020).

A parabolic-trough collector is a unified system consisting of two primary components: (i) parabolic-shaped mirrors and (ii) a receiver tube positioned along the focal axis of the parabola.

This design allows solar radiation that strikes the system in parallel to be concentrated at the focal point, as shown in the Figure 2.2.

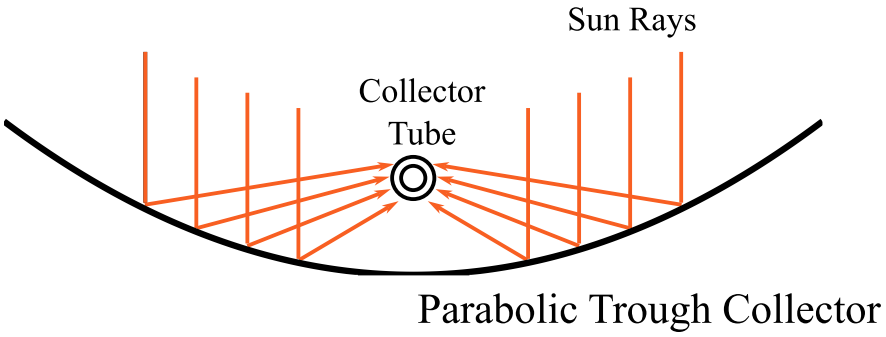

Figure 2.2: Diagram of operation of a parabolic-trough collector.

The focus of the parabola extends into a focal line along the length of the channel. A receiver tube is placed along this line, containing a thermal fluid (usually oil) that is heated as the tube absorbs the concentrated solar radiation.

The collection of radiant energy from the Sun is used for electric power generation or conversion to thermal energy for industrial processes. Solar thermal collectors may be used in low-temperature applications as in flat-plate collectors (less than 80°C) or of medium temperature with an optical concentration stage, in which the light first impinges on a reflecting surface and then it is redirected towards a receiving element with selective absorbing properties. Here, energy is transferred to a fluid—usually water—thus raising its temperature, and subsequently, it is stored in a thermally insulated tank (Los Santos-García et al., 2016).

Two main types of collectors without concentration are used for household processes (Pérez-Denicia et al., 2017). The first one is the flat-panel collector and the second one is the evacuated-tube collector; both collect direct and diffuse radiation. On the other hand, the main concentration systems are dish collector, parabolic trough, linear Fresnel configuration, and central receiver. Concentration

systems are used when the temperature to be achieved is beyond 150°C as in steam generation systems (Los Santos-García et al., 2016).

Due to their geometry, parabolic-trough collectors focus the incident radiation on a focal line, using evacuated tubes as receivers. This type of collector requires tracking the Sun in one axis; this increases its complexity and, consequently, the costs of initial investment, as well as operating and maintenance costs, in contrast to the flat-plate collector systems, which have no moving parts (AlZahrani and Dincer, 2018). For parabolic-trough geometry, a highly reflective aluminum sheet with surface-protective Alanod multilayer (Moghimi and Ahmadi, 2018) is commonly used in industrial concentrators. On July 11, 2012, it rounded costs of $58.50 per square meter. Besides, a supporting structure is needed, in which the aluminum sheet is placed with a Sun-tracking mechanism. Consequently, this system has mobile parts and high price and weight.

The Institute of Renewable Energy (IER) and the Electrical Research Institute (IIE), both in the state of Morelos in Mexico, have developed projects with parabolic-trough concentrators. Their manufacturing and materials costs reached $1706 per square meter A complete overview of parabolic-trough solar collectors and their applications can be found in the work reported by Erdenedavaa et al. (2018).

Most solar thermal applications for industrial processes have been installed on a relatively small scale and are mostly experimental. Only 85 solar thermal plants for processing heat were reported worldwide in 2008, with an installed capacity of 25 M $35,700m^2$ and with an average power of 320 K; the capacity of the systems was in the range between 50 K and 1.5 M. This 25 M capacity was a minuscule amount compared to the total industrial demand. Industrial applications typically require high temperatures and great volumes. Solar thermal systems, when correctly integrated into an industrial process, can provide increased energy efficiency and reduction of carbon-dioxide emissions (Los Santos-García et al., 2016).

Parabolic trough collectors can efficiently drive industrial processes that require medium-temperature heat, typically in the range of 150°C to 400°C. These processes include the production of hot water, low-enthalpy steam, and thermal energy for industrial heating applications. PTCs are widely used in sectors such as food processing, textile manufacturing, and chemical industries, where

medium-temperature heat is crucial for various production stages. The versatility of PTC designs allows for a broad range of industrial applications. Specific PTC models are optimized for delivering hot water and low-enthalpy steam, which are essential in sterilization, pasteurization, and other heat-demanding processes. These systems are often modular, with solar collection areas ranging from 2.5 to 5.0 m^2, making them scalable and adaptable to different industrial setups Los Santos-García et al. (2016).

Moreover, by integrating PTCs with existing industrial heating systems, companies can significantly reduce their reliance on fossil fuels, lower operational costs, and contribute to reducing greenhouse gas emissions, thus aligning with global sustainability goals Frein and Valenzuela (2018). Recent advancements in thermal storage and hybridization with conventional energy sources have further enhanced the reliability and efficiency of PTCs in industrial applications, extending their usability even in regions with intermittent solar resources Kalogirou (2009).

2.2 PTC and the problem of dust

To harness solar energy on Earth, two main types of technologies have been developed: photothermal conversion technologies and photovoltaic conversion technologies. Among the photothermal options, parabolic trough collectors stand out as the most advanced and widely used technology, contributing significantly to global concentrating solar power generation. Given their pivotal role, it is crucial to maintain PTCs in optimal working condition to ensure continuous high performance (ROJO, 2017).

Maintaining this performance begins with accurate prediction and optimization of the system's optical efficiency. This was achieved through finite element simulations, geometric measurements, and analysis of the optical properties of key components. The simulations included reflector deformations and receiver sag under various tracking orientations, while an elastostatics model characterized torsional deformations. Additionally, module alignment errors, slope deviations in the reflector layout, and bracket placement inconsistencies—based on typical manufacturing assembly—were incorporated into the analysis. Using a

Monte Carlo Raytracing software, the collected data on geometrical and optical inputs was combined with the physical properties of the receiver and reflectors to predict the overall optical efficiency of the system (ROJO, 2017).

Following the optical assessment, thermal performance testing was conducted at the Solucar Platform's HTF Test Loop facility. Using an oil-based heat transfer fluid at a nominal outlet temperature of $393°C$, the thermal tests validated the collector's capacity to increase fluid temperature under controlled conditions. This facility, originally designed to test a four-collector EuroTrough loop, was recently upgraded with the *CompoSol* expansion for qualifying larger aperture collectors and high-temperature heat transfer fluids. Thermal testing involved measuring temperature gains along the collector under specific flow rates, with each collector's performance evaluated individually to ensure that the nominal outlet temperature was consistently reached (AlZahrani and Dincer, 2018).

After the optical and thermal optimizations, a comprehensive startup procedure was implemented. The procedure involved incrementally raising the HTF temperature by $50°C$ and tracking the sun for at least four hours at each increment, ensuring the early detection of any potential issues related to thermal expansion or design flaws. This rigorous testing process accumulated over 500 hours of operational data, during which the real-world thermal power output was compared against model predictions. The successful correlation between predicted and actual performance confirmed the reliability of the PTC system at its nominal operating conditions of $393°C$ and 40 bar pressure (AlZahrani and Dincer, 2018).

Through these detailed optical, thermal, and operational procedures, the PTC system was thoroughly tested and optimized, ensuring its ability to harness solar energy efficiently for industrial and large-scale power generation applications.

2.2.1 Dust deposition effect

The efficiency of solar energy utilization and the subsequent production of thermal energy are closely linked to the optical properties of the collector. Critical factors, such as the transmissivity of the glass cover on the receiver tube and the reflectivity of the mirrors, are significantly impacted by the accumulation of

dust on these surfaces. In response to this issue, some power plants have begun implementing strategies to mitigate the negative effects that dust accumulation can have on the overall performance of the power plant. These strategies aim to maintain the optimal functionality of the collectors, ensuring consistent energy output.

To assess how much the presence of dust affects, different studies have been carried out; for instance, in the work presented by Şahin (2007), the authors have observed a reduction of between 10% to 60% in the transmittance of the glass plates of several photovoltaic modules. As expected, an increase in the amount of dust produces a drop in the transmittance, which consequently leads to a drop in the power generated, as in the work presented in Ghazi et al. (2014), where the authors have reported a decrease of up to 60% of the energy produced. Given this problem, some strategies have been proposed to determine the level of dust, in such a way that it is possible to take actions that avoid significant drops in energy production.

2.2.2 Characterization of Dirtiness

Dust accumulation on the surfaces of parabolic trough collectors (PTCs) poses a significant challenge to their efficiency in capturing solar energy. PTCs depend on their mirrors to reflect sunlight onto a receiver tube, where the energy is concentrated to generate heat. However, when dust settles on these reflective surfaces or the glass covering the receiver tube, the system's optical performance is degraded. Dust particles cause light scattering and absorption, reducing the reflectivity of the mirrors and diminishing the intensity of the sunlight reaching the receiver. This reduction in optical efficiency lowers the thermal output, resulting in less electricity generated from the same amount of solar energy. In regions prone to frequent dust storms or high levels of particulate matter in the air, the impact is even more severe. Moreover, constant cleaning, which is necessary to maintain efficiency, leads to higher operational costs and increased water usage, making it essential to develop strategies for efficient dust monitoring and management.

Digital image processing offers an efficient way to address this issue by monitoring dust levels in real time. One promising method is to use histogram analysis

of images captured from the mirrors and receivers (Yfantis and Fayed, 2014). A histogram is a graphical representation of the intensity distribution of pixels in an image, which can reveal variations in brightness caused by dust accumulation. Clean mirrors or receiver tubes exhibit bright, uniform histograms with high pixel intensity values, while dust-covered surfaces show a shift in the histogram towards lower intensity values due to reduced reflectivity. By tracking these changes over time, operators can quantify the amount of dust present and determine when cleaning is necessary. This method can be highly effective in environments where manual inspections are impractical or too costly. Implementing an image-based dust monitoring system allows for more efficient use of resources, reducing the need for frequent cleaning and preventing efficiency losses without requiring constant human oversight.

While histogram analysis provides a simple and effective method for detecting dust, deep learning techniques, particularly convolutional neural networks (CNNs), offer an alternative and more advanced approach. CNNs are a type of deep learning model specifically designed for image recognition and analysis. In this context, CNNs can be trained to detect and classify varying levels of dust accumulation on PTC surfaces by learning patterns and features from large datasets of images. Unlike histogram analysis, which relies on changes in pixel intensity distribution, CNNs can capture more complex and subtle features such as dust particle size, distribution patterns, and different lighting conditions, which might be challenging to detect with traditional methods.

The advantage of using CNNs lies in their ability to generalize better across different conditions, such as varying light angles, weather conditions, and mirror degradation over time. For instance, CNNs can be trained to differentiate between shadows, dirt, and actual dust accumulation, providing more accurate assessments than histogram-based methods. Additionally, CNNs can automate the process of not only detecting dust but also predicting future cleaning needs based on environmental data, integrating weather forecasts, and historical performance metrics. However, this approach requires a larger dataset for training and significantly more computational power compared to histogram analysis, which is simpler and easier to implement in real time.

In conclusion, both histogram analysis and CNNs offer valuable solutions for monitoring dust accumulation in PTC systems. Histogram analysis provides a straightforward, low-cost method for real-time dust detection and is suitable for basic applications with limited computational resources. On the other hand, CNNs provide a more sophisticated, robust approach that can handle complex conditions and yield higher accuracy, though at the expense of requiring more data and computational power. Depending on the specific needs and resources of a solar power plant, either technique could be employed to maintain high efficiency and reduce the negative impacts of dust deposition on solar energy generation.

2.3 Deep learning-based image analysis

Deep learning-based image analysis refers to the use of deep neural networks, specifically CNNs, to automatically analyze and interpret images (Wei et al., 2021). Unlike traditional image processing methods that rely on predefined algorithms (such as edge detection or histogram analysis), deep learning models learn patterns and features directly from raw image data. These models are composed of multiple layers of artificial neurons, where each layer learns increasingly abstract features of the image—starting from simple patterns like edges and textures in the early layers, to more complex objects and relationships in deeper layers.

A key strength of deep learning for image analysis lies in its ability to learn from large datasets and generalize across different conditions. CNNs, for instance, can be trained to identify objects, classify images, segment regions of interest, or even detect subtle variations such as different levels of brightness or texture. One of the most common applications is object recognition, where a trained CNN can accurately identify objects within an image, regardless of changes in orientation, lighting, or background. Another important use case is image segmentation, where deep learning can be applied to label every pixel in an image, separating foreground objects from the background or different regions within an object (Alzubaidi et al., 2021).

Deep learning-based image analysis is highly effective in fields such as medical imaging, where CNNs can be trained to detect tumors or abnormalities in X-

rays or MRIs. Similarly, in autonomous driving, deep learning models are used to interpret real-time images from cameras, detecting pedestrians, vehicles, and road signs. These models also excel in more creative applications, such as style transfer, where the model learns to recreate an image in the style of a famous painting, or in image restoration, where CNNs can remove noise or recover missing parts of an image.

2.3.1 Neural Network

A neural network is a simplified model that emulates how the human brain processes information. Works by combining a significant number of interlinked processing units that look like abstract versions of neurons IBM (2020).

The processing units are organized in layers. There are normally three parts in a neural network: an input layer with units that represent the entry fields, one or several hidden layers, and an output layer with one or several units that represent the target field(s). The units are connected with variable connecting forces (or weightings). The input data are presented in the first layer, and the values are propagated from each neuron to each neuron of the subsequent layer. In the end, a result is sent from the output layer. Figure 2.3 shows the basic diagram of a neural network IBM (2020).

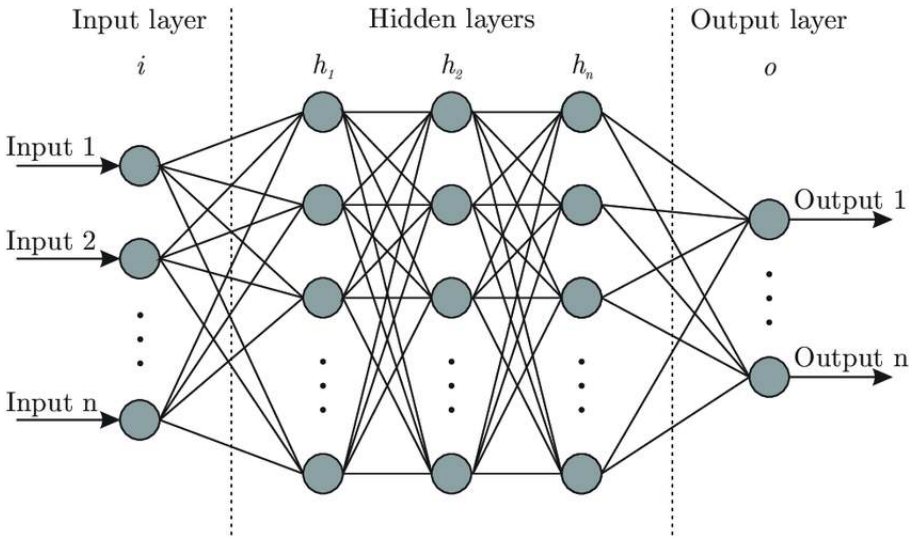

Figure 2.3: Simple Neural Network

The neural network learns by examining the individual records, generating a prediction for every record, and making adjustments to the weightings whenever such a prediction is wrong. This process is performed repeatedly and the network still improves its predictions until reaches one or several stopping criteria Medsker and Jain (2001). Examples in which the result is known are continuously presented to the network and the responses provided are compared to the known results. The information from this comparison is passed backward through the network gradually changing the weightings. As training progresses, the network becomes more accurate every time in the replication of known results.

Once the network is trained, can be applied in future cases in which the result is unknown Bertozzi et al. (2002).

2.3.2 Convolutional Neural Network

A Convolutional Neural Network is a model specifically designed for processing structured grid data, such as images. CNNs are particularly well-suited for image analysis tasks because they automatically learn spatial hierarchies of features, starting from low-level patterns like edges and textures, to more complex structures like shapes and objects, through a process called convolution. This architecture mimics how the human visual system works, making CNNs highly effective for tasks like image recognition, classification, object detection, and segmentation (Dhruv and Naskar, 2020).

The core building blocks of a CNN include convolutional layers, pooling layers, and fully connected layers. In a convolutional layer, filters (or kernels) slide across the input image, performing a mathematical operation called convolution. Each filter detects specific features such as edges, corners, or textures by transforming small regions of the image into feature maps. These feature maps capture the presence of certain patterns, which are then passed on to the next layer. Through multiple layers of convolution, the CNN learns more abstract and high-level representations of the image, such as specific objects or parts of objects.

Pooling layers, often placed between convolutional layers, are used to reduce the spatial dimensions of the feature maps, making the network more computationally efficient and reducing the risk of overfitting. Pooling typically takes the

form of max pooling, where only the most significant value within a small region is retained, allowing the network to focus on the most prominent features while discarding irrelevant details. This process reduces the complexity of the data while preserving key information.

At the end of the network, fully connected layers are used to make final predictions. The outputs from the convolutional layers are flattened into a single vector, which is fed into one or more fully connected layers. These layers combine the high-level features extracted from the earlier layers to perform tasks such as classifying the image into categories, detecting objects, or recognizing patterns. In image classification, for instance, the final layer assigns a probability score to each possible class, and the class with the highest score is chosen as the network's prediction. Figure 2.4 shows the general form of a CNN model.

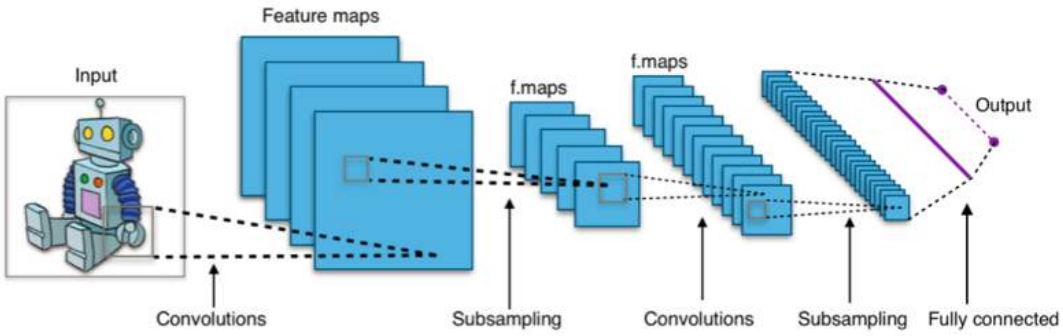

Figure 2.4: General CNN architecture.

CNNs are widely used in a variety of applications, for instance, to improve the accuracy on electric power bushing identification based on images where a novel algorithm was developed, building upon the YOLOv2 network Huang et al. (2021), to enhance the recognition performance of these images. While YOLOv2 is a powerful convolutional neural network, it has limitations in handling rotated objects and to solve this problem, the standard Hough transform and image rotation are utilized to determine the optimal recognition angle for target detection, such that an optimal recognition effect of YOLOv2 on inclined objects (for example, bushing) is achieved. To overcome the rotation in-variance issue, the Hough transform and image rotation techniques were employed to identify the ideal. Concerning the problem that the bounding box is biased, the shape

feature of the bushing is extracted by the Gap statistic algorithm, based on K-means clustering; thereafter, the sliding window (SW) is utilized to determine the optimal recognition area. To address the bias in bounding box generation, the Gap statistic algorithm and K-means clustering were used to analyze the shape characteristics of the bushings. Subsequently, the sliding window technique was implemented to pinpoint the most suitable recognition region, further refining the detection process. Experimental verification indicates that the proposed rotating image method can improve the recognition effect, and the SW can further modify the BB. The accuracy of target detection increases to 97.33%, and the recall increases to 95% Zhao and Zhang (2020).

3

Methodology

This chapter details the research design, data collection techniques, and analytical tools used to address the objectives of the study. Particularly, a two-step approach has been implemented. First, high-resolution images of the collector are captured. In the second step, image processing algorithms are applied to these images to identify and quantify the extent of dust deposition.

3.1 Image analysis

In this section, we outline the implemented approach for classifying dust particles, see Figure 3.1, the proposed methodology consists of three stages.

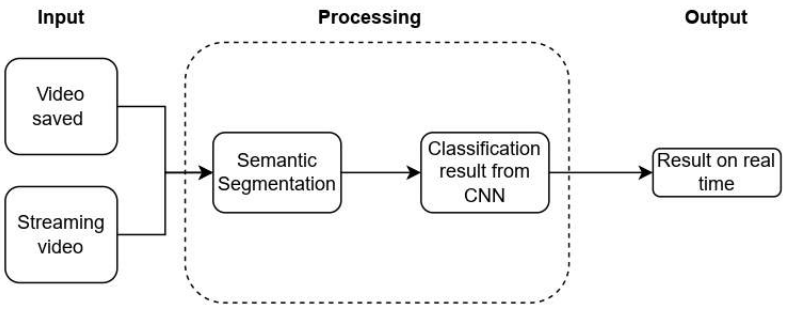

Figure 3.1: Methodology used during the realization of this work.

In the initial phase, UAVs were used to capture images of the parabolic-trough collector. Subsequently, in the second stage, a semantic segmentation of the ROI

is performed, and a perspective transformation was applied to ensure that only pertinent information was utilized and that the images were standardized in terms of pixel dimensions. Then in the third the classification results were obtained by mean of the implemented CNN.

A more detailed explanation of each stage is presented in the following sections.

3.1.1 Image acquisition

Several images with different levels of dirt and at different times of day were taken using a drone DJI Matrice 100 (DJI, 2021) and a DJI-Zenmuse Z3 camera, equipped with a 3.5x optical zoom and a 12-megapixel image resolution. After this, it was performed a perspective transformation to the images in Python, and the image processing was carried out on OpenCV (Library, Open Source Computer Vision, 2020), so as to homogenize the dimensions and turn them easy to study. Subsequently, the images were processed, following two approaches: digital image processing and deep learning-based analysis.

A dataset of 3,500 images was collected, capturing various dust levels and different times of day. Figure 3.2 shows some of the images acquired with the UAV.

3.1.2 ROI extraction

Following image acquisition, a ROI was extracted, specifically focusing on the receiver tube. This step was taken to isolate pertinent information from the PTC. Given that the captured images were often non-rectangular, a manual perspective transformation was implemented to ensure that the image set used in subsequent processes maintained consistent dimensions in terms of pixel count.(487×125). In Figure 3.3 the ROI as well as the perspective transformation can be appreciated.

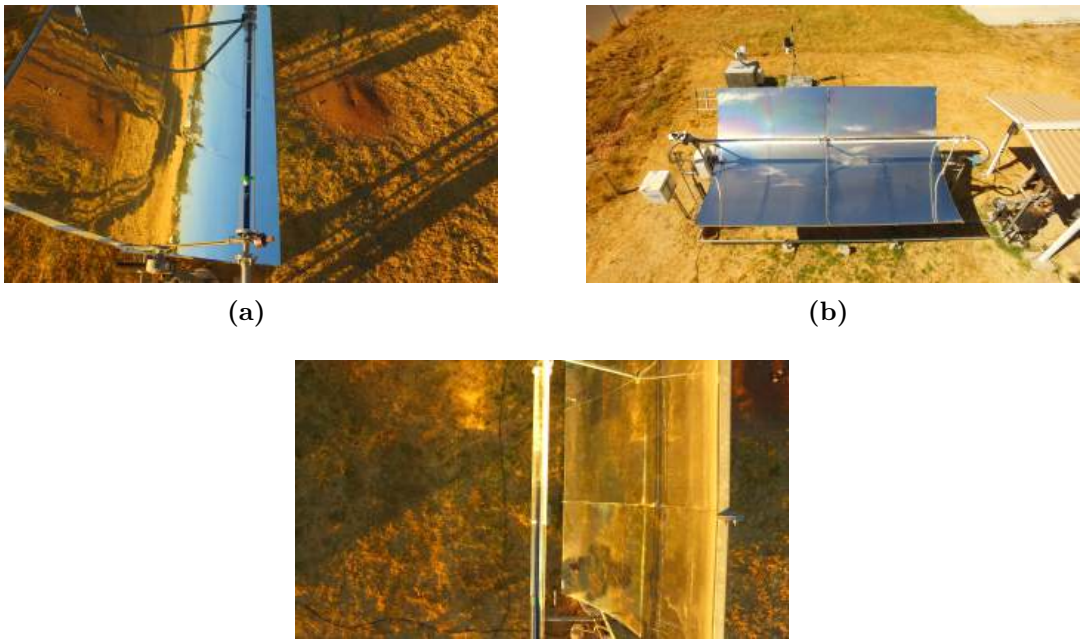

(a) (b)

(c)

Figure 3.2: Example of images acquired by UAV..

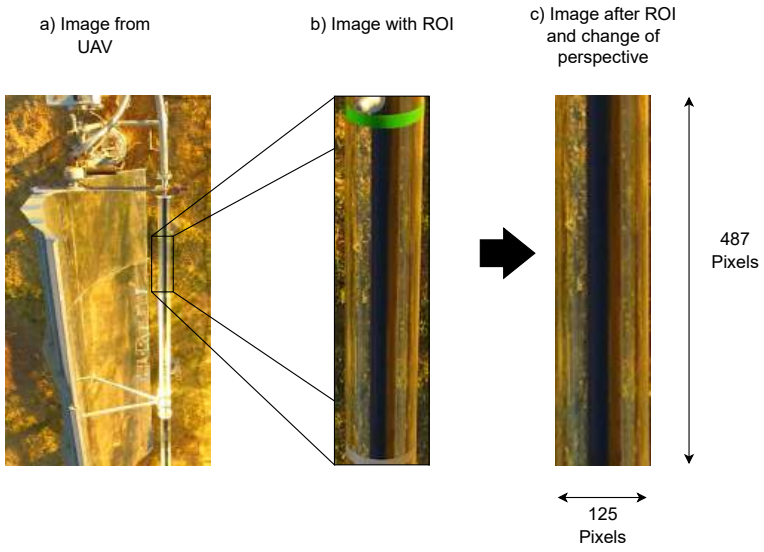

Figure 3.3: Preprocessing of the parabolic-trough collector images

3.1.3 Automatic ROI extraction

To effectively obtain the ROI automatically, a UNet architecture (Ahmad et al., 2021; Ronneberger et al., 2015) has been implemented. In particular, the methodology to be followed is the one proposed in Figure 3.4.

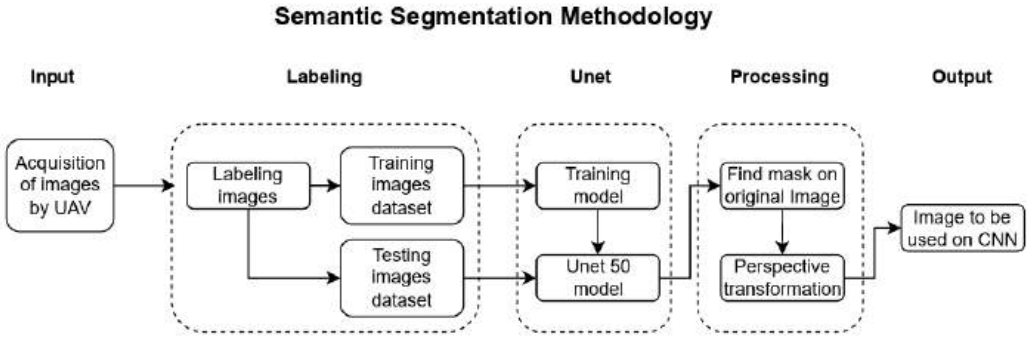

Figure 3.4: Methods for Segmentation Semantic Neural Network

The U-Net architecture comprises two primary processes. The first process, known as contraction or encoding, is responsible for capturing the contextual information within an image. This process involves a series of convolutional and max-pooling layers, which enable the creation of a map of the image's characteristics while simultaneously reducing its size to optimize the number of network parameters (Ahmad et al., 2021).

The second process is the symmetric expansion, also known as "decoding", which enables precise localization through transposed convolution The architecture of the neural network that was proposed in this work is the one described in Figure 3.5.

The segmented image produced by the U-Net enables the automated detection of the collector and subsequent analysis of its dust level. Figure 3.6 shows the segmentation process.

3.1.4 Labeling

To train the classifier effectively, each image was manually categorized based on its dust level. Four distinct dust levels were defined: clean, middle1, middle2,

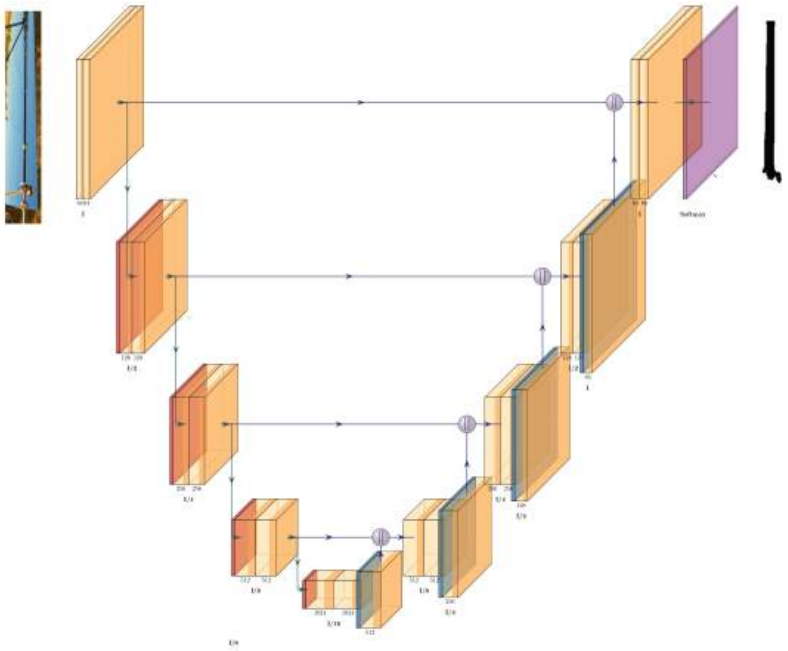

Figure 3.5: U-Net architecture.

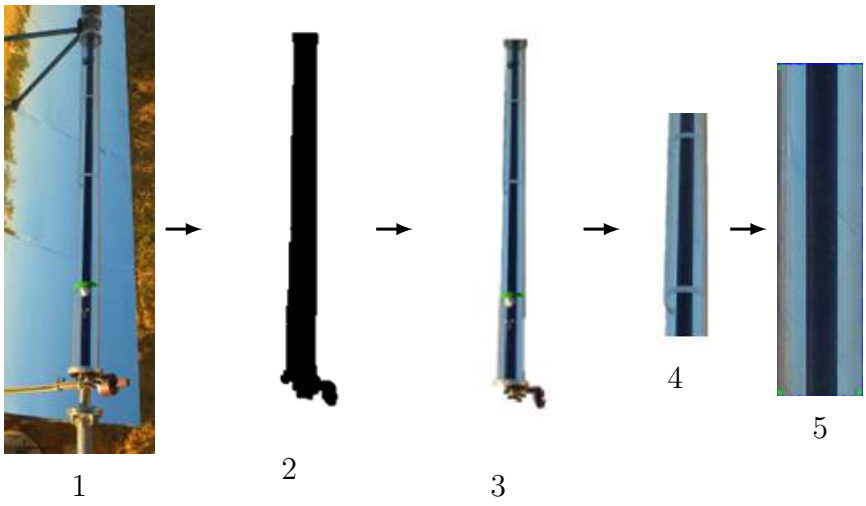

Figure 3.6: ROI segementation. (1) Input image. (2) Obtained Mask. (3) Located the mask in the original image. (4) Section with area of 36,000 pixels. (5) Perspective transformation.

and dirty. Subsequently, the images were divided into training and test groups to ensure that the classifier could be evaluated with unseen images, allowing for

accurate validation.

Characteristic images of each class are shown in Figure 3.7.

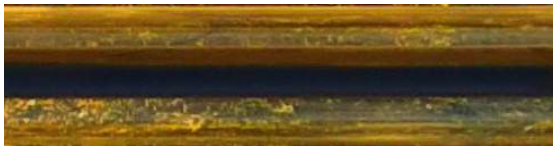

(a)

(b)

(c)

(d)

Figure 3.7: Example of images labeled. Each image corresponds to each of the four classes (clean, middle1, middle2, and dirty)

To enhance model training, a data augmentation process was implemented, generating "new" images through various transformations, including rotation and movements along both the horizontal and vertical axes (Taqi et al., 2018). Figure 3.8 shows some images resulting from this process.

The resulting dataset is made up of 3,100 images, of which there are 775 images per class.

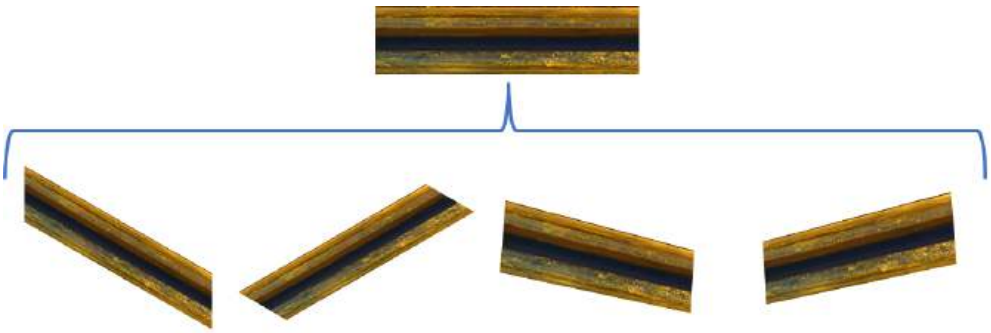

Figure 3.8: Example of images resulting from data augmentation process.

3.1.5 CNN model

A neural network (NN) can be employed for dust classification, it necessitates the definition and extraction of a set of features. This approach, however, may not be optimal as it involves mapping a two-dimensional object (image) into a one-dimensional representation. Such a transformation can lead to drawbacks, such as the loss of spatial information within the image. An alternative approach to addressing the classification problem involves the utilization of Convolutional Neural Networks (CNNs). CNNs have demonstrated remarkable effectiveness, particularly in the realm of image-related tasks. Their applications encompass image classification, image semantic segmentation, and object detection within images, among others. This efficacy can be attributed to their architectural design, which is specifically tailored to handle three-dimensional objects. This is exemplified by color images, where each channel can be interpreted as a distinct dimension.

To classify the dust levels, a deep learning approach was proposed, specifically utilizing a Convolutional Neural Network.

The proposed CNN (see Figure 3.9) is made up of an input layer of 514,650 flat neurons (this corresponds to the number of pixels that each of the images has), followed by a layer of convolution (Kembuan et al., 2020). This layer applies a kernel (a small, learned filter) to the input image, sliding it across the image and producing an output tensor. This process is known as convolution (Kembuan et al., 2020). Subsequently, a *Max-polling* layer is employed. This layer is designed to extract the most significant information from each image while reducing its

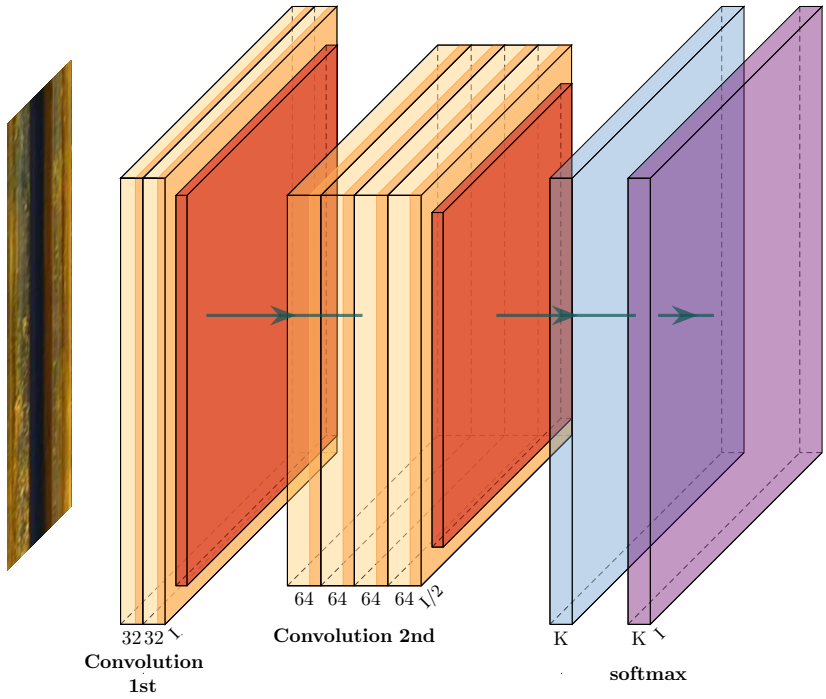

Figure 3.9: Architecture of the proposed CNN.

size. It achieves this by analyzing 2x2 pixel neighborhoods and preserving the pixel with the highest value.Hussain et al. (2018).

Following this, another convolutional layer is introduced, this time utilizing 64 kernels. Subsequently, another *Max-polling*layer is applied, further reducing image size and extracting only the most critical information, thereby optimizing the training process within the hidden layers. There are two hidden layers, each consisting of 100 neurons (Hussain et al., 2018).

The optimization model used is *Adam* (Meng et al., 2017) since it allows efficient computing in terms of memory and it is optimized on solving issues with large amounts of data as the images are. Finally, as output a *softmax* layer is implemented.

The softmax function takes as input a vector z of K real numbers, and normalizes it into a probability distribution consisting of K probabilities proportional to the exponential of the input numbers, in this case $K = 4$.

As previously noted, all images used to train the CNN model must have consistent dimensions in terms of pixel count. Furthermore, the images are converted to floating-point format and normalized to facilitate effective learning (Meng et al., 2017).

3.2 Graphical user interface

To have an easy way to use the trained models of both U-Net for the collector localization and CNN for the dust classification, it was decided to make a graphical user interface (GUI) that was developed in Python (Foundation, The Python Software, 2020). The interface is capable of both analyzing a saved video or acquired real time images.

The implemented GUI is depicted in Figure 4.2. As it may be observed, the output of the GUI shows the identification of the dust level per area is shown by a box drawn on the video/image with a legend that describes the level of dust that is being detected.

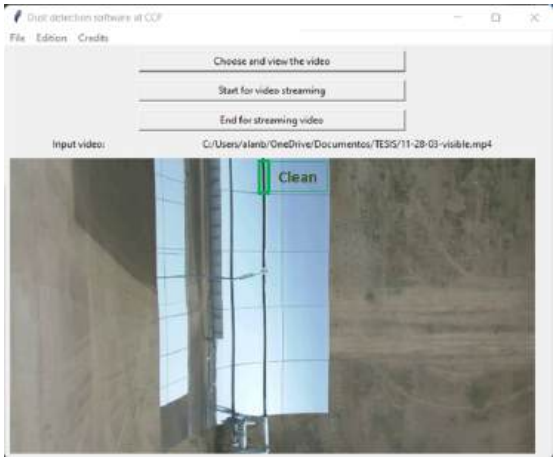

Figure 3.10: Caption

The implementation of a GUI for the dust classification problem in parabolic trough collectors (PTCs) is essential to enhance usability, streamline analysis, and facilitate decision-making for non-expert users. A GUI provides an intuitive platform for operators and engineers to analyze images of dust deposition without

needing extensive technical knowledge of image processing techniques. By incorporating user-friendly features such as automated dust classification algorithms, and visual displays of results, the GUI simplifies complex tasks like detecting dust accumulation patterns and assessing their impact on collector performance. Overall, the GUI bridges the gap between advanced image analysis techniques and practical, day-to-day management of PTC systems.

3.3 Performance metrics

A confusion matrix is a tabular representation used to evaluate the performance of classification algorithms by displaying the relationships between actual and predicted classes. Each row of the matrix represents the instances in an actual class, while each column represents the instances in a predicted class. The diagonal elements of the confusion matrix represent the number of instances where the predicted class matches the actual class (i.e., correctly classified instances), while the off-diagonal elements indicate misclassifications, where the predicted class differs from the actual class.

For a multi-class problem with n classes, the confusion matrix is an $n \times n$ matrix, where each row corresponds to the actual class, and each column represents the predicted class. The elements of the matrix, denoted as M_{ij}, represent the number of instances where the true class was i and the predicted class was j. In this way, the diagonal elements M_{ii} show the number of correct predictions for each class, while the off-diagonal elements represent the misclassifications. Table 3.1 shows the confusion matrix structure for a multi-class classification

	Predicted A	**Predicted B**	**Predicted C**
Actual A	TP (A)	FP (B)	FP (C)
Actual B	FN (A)	TP (B)	FP (C)
Actual C	FN (A)	FN (B)	TP (C)

Table 3.1: Confusion Matrix for Multi-Class Classification

problem with three classes (A, B, and C). From this table, TP (True Positives) denotes the correctly classified instances for a given class (on the diagonal), FP

(False Positives) are the instances that were incorrectly classified as a different class, and FN (False Negatives) indicates the instances of a class that were misclassified as another class.

3.3.1 Performance Metrics from the Confusion Matrix

Several performance metrics can be derived from the confusion matrix, allowing for a more detailed evaluation of the classifier's performance across all classes:

- **Accuracy**: The overall accuracy of the model is defined as the ratio of correctly predicted instances (sum of the diagonal elements) to the total number of instances. Mathematically, it is expressed as:

$$\text{Accuracy} = \frac{\sum_{i=1}^{n} M_{ii}}{\sum_{i=1}^{n} \sum_{j=1}^{n} M_{ij}}$$

  However, accuracy can be misleading when dealing with imbalanced datasets, where some classes have more instances than others.

- **Precision, Recall, and F1-Score**: These metrics are typically calculated for each class individually.

  - Precision for class i is the ratio of correctly predicted instances of class i to all instances predicted as class i:

$$\text{Precision}_i = \frac{M_{ii}}{\sum_{j=1}^{n} M_{ji}}$$

  - Recall (or sensitivity) for class i is the ratio of correctly predicted instances of class i to all instances that actually belong to class i:

$$\text{Recall}_i = \frac{M_{ii}}{\sum_{j=1}^{n} M_{ij}}$$

  - F1-score for class i is the harmonic mean of precision and recall, providing a balanced measure:

$$\text{F1-Score}_i = 2 \times \frac{\text{Precision}_i \times \text{Recall}_i}{\text{Precision}_i + \text{Recall}_i}$$

The confusion matrix thus provides a comprehensive way to visualize and measure the performance of a multi-class classifier, offering insights into not just overall accuracy but also the specific areas where the model may be underperforming, such as misclassifications between certain classes.

4

Results

The results section presents the performance analysis of the convolutional neural network (CNN) model applied to the dust classification problem in parabolic trough collectors (PTCs). Through a series of experiments, the model was trained and tested on a dataset of images capturing various levels and patterns of dust deposition on PTC surfaces. The section explores key performance metrics, including accuracy, precision, recall, and F1-score, for multiple dust categories, providing insights into the CNN's ability to distinguish between different dust levels. Additionally, confusion matrices and visualizations of misclassified samples are analyzed to assess the strengths and weaknesses of the model.

The proposed methodology has been implemented using Python as the programming language, and the libraries used were *Tensorflow* (TensorFLow, 2021) for the Convolutional Neural Network and UNet architectures and *OpenCV* (Library, Open Source Computer Vision, 2020) for the digital image processing.

4.1 Training results

During the training stage of the U-Net network for dust classification, the model's performance was tracked using two key metrics: the loss function and Intersection over Union (IoU). The training curve for the loss function showed a consistent downward trend as training progressed, indicating that the model was effectively minimized the error between the predicted and actual segmentations of dust regions. At the beginning of training, the loss decreased monotonically and rapidly,

implying that the model converged. Similarly, the intersection over union (IoU) metric, which measures the overlap between predicted and true dust regions, improved steadily throughout the training. Initially, the IoU values were low, reflecting poor segmentation, but as the model learned from the data, the IoU increased, approaching higher values that indicated more accurate dust segmentation. The combination of decreasing loss and increasing IoU over epochs suggests that the U-Net network was learning to effectively capture and segment dust patterns on the parabolic trough collectors. In Figure 4.1 the training behavior of the U-Net model is shown.

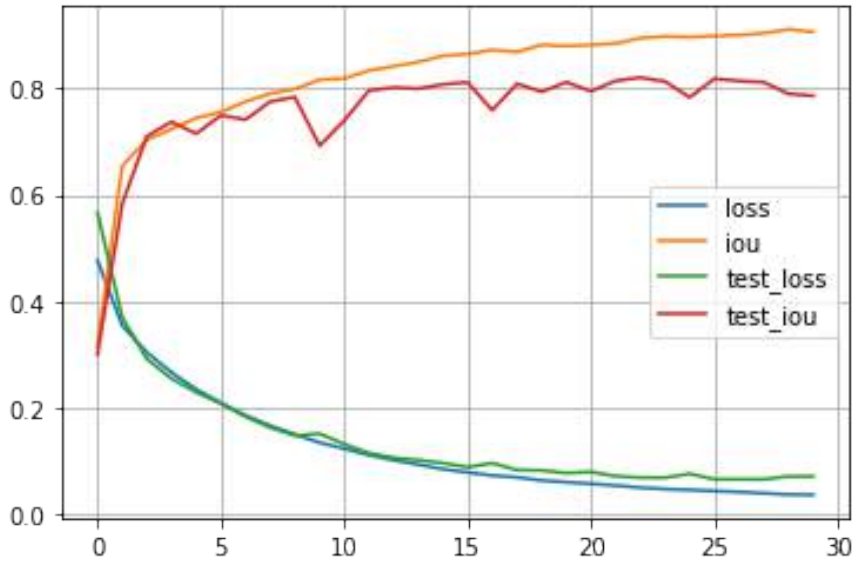

Figure 4.1: Loss and IoU behavior during training.

In contrast, during the training stage of the CNN classification network for dust classification, the model's performance was evaluated using the loss-accuracy training curve. Initially, the loss decreased rapidly as the model adjusted its weights, indicating that it was learning to minimize the error between predicted and actual class labels. This sharp drop in loss was accompanied by a corresponding increase in accuracy, as the network began to correctly classify a greater proportion of dust images. Over time, the loss continued to decline at a slower rate as the model neared convergence. Meanwhile, accuracy showed a steady upward trend, with occasional fluctuations due to the learning process. These

fluctuations typically occurred in the earlier epochs but stabilized in later stages, reflecting the model's increasing generalization capabilities. By the end of the training, the network demonstrated high accuracy and low loss, signifying that the CNN effectively learned to classify different dust levels in the images.

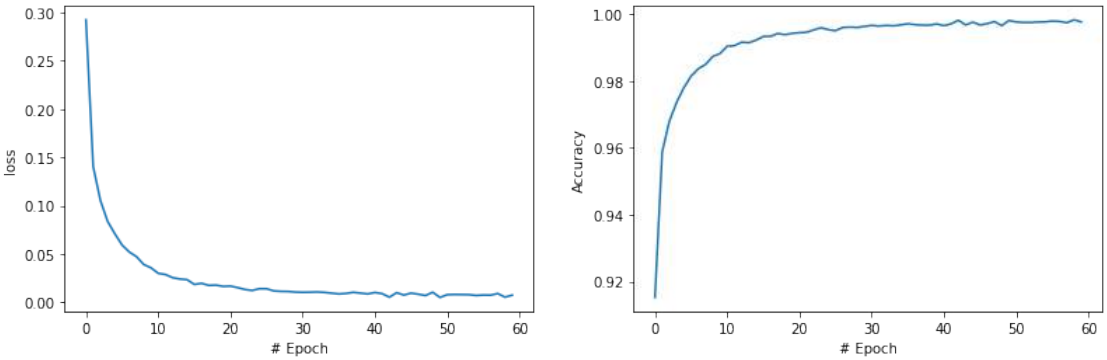

(a) **(b)**

Figure 4.2: Training stage behavior of the CNN. (a) Loss vs #Epochs. (b) Accuracy vs #Epochs.

4.2 Dust classification results

The results of the CNN classification model for dust classification are presented in this section, highlighting the model's ability to distinguish between various levels of dust accumulation on parabolic trough collectors. The CNN was evaluated using multiple performance metrics, including accuracy, precision, recall, and F1-score, to assess its classification capabilities. The results are further illustrated through confusion matrices that reveal how well the model differentiates between different dust categories. Additionally, misclassifications are analyzed to identify common errors and potential improvements.

The classification report of the CNN model, presented in Table 4.1, provides a detailed breakdown of the model's performance across four different classes: "Clean", "Middle 1", "Middle 2", and "Dirty". The table includes key metrics such as precision, recall, F1-measure, and support for each class.

Table 4.1: Classification report of the CNN model.

Class	Precision	Recall	F1-Score	Support
Clean	0.960	0.960	0.960	25
Middle 1	0.913	0.840	0.875	25
Middle 2	0.821	0.920	0.868	25
Dirty	0.958	0.920	0.938	25
Accuracy			0.91	100

For the "Clean" class, the model achieved a high precision, recall, and F1-measure of 0.960, indicating that it can accurately identify clean surfaces with minimal false positives and false negatives. The performance for the "Dirty" class is also strong, with an F1-measure of 0.938, supported by high precision (0.958) and recall (0.920), showing that the model is effective at detecting dirty surfaces.

The "Middle 1" and "Middle 2" classes represent intermediate levels of dust, and the model's performance for these classes is slightly lower. For "Middle 1", the F1-measure is 0.875, with a precision of 0.913 and a recall of 0.840, indicating that the model is better at predicting this class than detecting it. In contrast, for "Middle 2" the recall (0.920) is higher than the precision (0.821), suggesting that the model is more sensitive to identifying this class but generates more false positives.

Overall, the model achieved an accuracy of 0.91 across all classes, demonstrating strong classification performance. The slight variations in precision, recall, and F1-measure between the "Middle" classes highlight potential areas for improvement, particularly in distinguishing between intermediate levels of dust accumulation. However, the high overall accuracy and strong performance in detecting the extremes ("Clean " and "Dirty") indicate that the CNN model is effective for the dust classification task.

Similarly, the confusion matrix depicted in Figure 4.3 illustrates the performance of the CNN model in classifying dust levels across the four categories ("Clean", "Middle 1", "Middle 2", and "Middle 3"). As mentioned, each cell in the matrix represents the proportion of predictions made by the model for a given class, relative to the actual class.

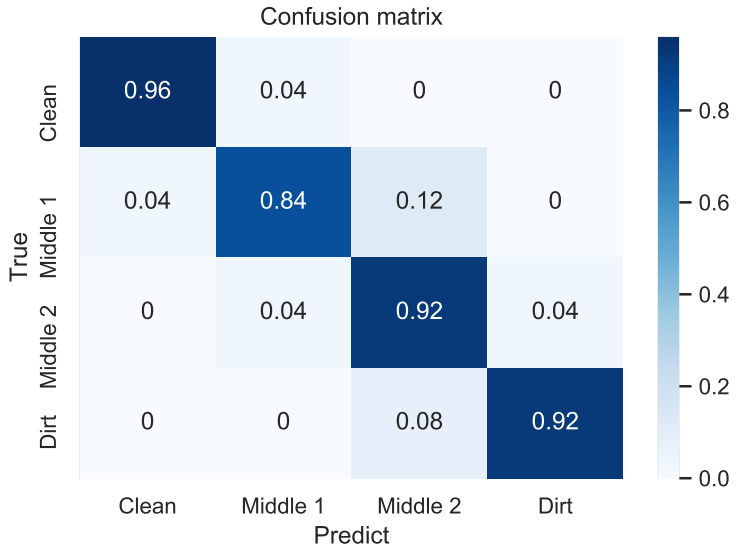

Figure 4.3: Classification confusion matrix.

For the "Clean" class, the model performs exceptionally well, with 96% of the "Clean" samples being correctly classified. Only 4% were misclassified as "Middle 1", and none were misclassified into higher dust levels, showing that the model has a high precision for identifying "clean surfaces".

The "Middle 1" class shows some confusion with both "Clean" and "Middle 2". While 84% of the samples were correctly classified, 4% were misclassified as "Clean" and 12% as "Middle 2". This indicates some overlap in the model's ability to distinguish between the lower and middle dust levels.

For the "Middle 2" class, the model achieves 92% accuracy, but 4% of samples were confused with "Middle 1" and another 4% with "Middle 3". This suggests that the model struggles slightly with distinguishing between the adjacent levels of dust accumulation.

The "Middle 3" class has a high classification accuracy of 92%, with only 8% of instances being misclassified as "Middle 2". This performance suggests that the model is more effective at classifying the higher dust levels, but still has some difficulty in precisely distinguishing between the "Middle" dust categories.

Overall, the confusion matrix reveals strong classification performance for the "Clean" and "Middle 3" classes, while the "Middle 1" and "Middle 2" classes show

a degree of confusion, particularly between adjacent dust levels. This suggests that further refinement may be needed in the model to improve its ability to differentiate between intermediate dust categories. For instance, to enhance the model's performance, increasing the database size or refining the criteria used to define each class could be considered.

4.2.1 Three Levels of Dust Classification

The use of three levels of dust classification ("Clean", "Middle", "Dirt") instead of four ("Clean", "Middle 1", "Middle 2", "Dirt") simplifies the problem and offers practical advantages without sacrificing the operational usefulness. First, merging the intermediate levels simplifies decision-making, as the distinction between slightly dusty (Middle 1) and moderately dusty (Middle 2) surfaces often does not result in different maintenance actions. A single "Middle" category still captures the necessary gradations between clean and heavily soiled collectors, while minimizing confusion. Additionally, reducing the number of classes improves the robustness of the classification model, lowering the risk of misclassification and increasing overall accuracy. Operational relevance is another key factor; real-world applications benefit from clear thresholds between clean, moderately dusty, and heavily soiled surfaces, without the need for more granular categories that offer little practical benefit. Lastly, the use of three levels instead of four reduces computational complexity, resulting in faster training times and more efficient model deployment. Figure 4.4 shows the model performance in terms of the confusion matrix when merging the two intermediate dust levels, "Middle 1" and "Middle 2", into a single "Middle" class.

The fusion of "Middle 1" and "Middle 2" into a unified "Middle" class shows some interesting shifts. First, the model correctly classifies 88% of "Middle" cases. 4% of the "Middle" instances are misclassified as "Clean", and only 2% as "Dirt". This misclassification toward "Clean" could indicate that borderline "Middle" cases, particularly those closer to "Middle 1", resemble clean surfaces optically. The slight 2% misclassification as "Dirt" suggests that a small portion of moderately dusty surfaces may exhibit characteristics of heavily soiled ones, though this error is minimal.

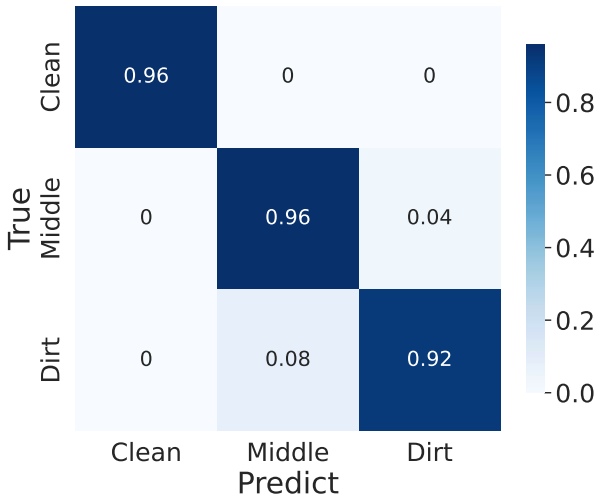

Figure 4.4: Classification confusion matrix with three dust levels.

In summary, the fusion of the intermediate classes into a single "Middle" category simplifies the classification problem, reducing complexity without sacrificing significant performance. This adjustment improves the model's robustness in cases where the distinction between adjacent dust levels ("Middle 1" and "Middle 2") may not be crucial for practical purposes, such as determining cleaning schedules. By focusing on three clear categories, the model can more effectively support decision-making in maintenance operations.

5

Conclusions and Recommendations

5.1 Conclusions

The research presented in this work has laid a solid foundation for the development of a robust dust classification system in parabolic trough collectors which was addressed in two main stages: the automatic segmentation of ROI using a U-Net network and the subsequent classification of the segmented ROIs into four dust levels using a CNN.

In the first stage, the U-Net network was employed to automatically segment the ROI, identifying the areas of the collector surfaces where dust deposition was present. This segmentation was essential for isolating relevant regions for further analysis, ensuring that only the surfaces of interest were considered in the classification stage. The performance of the U-Net, as measured by metrics such as Intersection over Union (IoU) and loss, showed that the network was effective in accurately identifying dust-covered regions, providing a reliable foundation for the subsequent classification task.

The second stage involved classifying the segmented ROI into four dust levels: “Clean”, “Middle 1”, “Middle 2”, and “Middle 3”. This was achieved using a CNN, and the results, as presented in the confusion matrix, demonstrate the model’s strong performance overall. The CNN achieved high classification accuracy for extreme dust levels, with 96% accuracy for the “Clean” class and 92%

for the “Middle 3” class. However, intermediate dust levels, such as “Middle 1” and “Middle 2”, exhibited some misclassification. Specifically, 12% of “Middle 1” instances were classified as “Middle 2”, and “Middle 2” was misclassified as ”Middle 1” and “Middle 3” at a rate of 4% each. This suggests that while the model effectively distinguishes between very clean and very dirty surfaces, it encounters difficulties in differentiating between adjacent intermediate levels of dust.

The implementation of a GUI is crucial for translating these advanced technical methods into a user-friendly tool for operators in solar energy plants. A GUI allows non-expert users to seamlessly input images, view the results of automatic segmentation, and classify dust levels with minimal effort. This simplifies the process of monitoring dust deposition and optimizes cleaning schedules by providing real-time feedback on collector surface conditions. The GUI not only enhances accessibility but also improves operational efficiency by integrating the model’s capabilities into practical, day-to-day plant management.

In summary, the combined approach of automatic segmentation and classification successfully addresses the dust deposition problem in parabolic trough collectors, providing a reliable system for detecting and categorizing dust accumulation. While the model performs well overall, improvements in distinguishing between intermediate dust levels would enhance its robustness, particularly for optimizing cleaning schedules in solar energy systems.

The implementation of this system can significantly enhance the efficiency and longevity of parabolic-trough collectors, essential components of solar thermal power plants. By accurately monitoring and addressing dust accumulation, operators can optimize collector performance, reduce maintenance costs, and maximize energy output.

Future research could explore the following areas to further refine and expand the capabilities of the dust classification system:

- Real-time monitoring: Integrating the system with real-time data acquisition and analysis can enable operators to proactively address dust accumulation issues, preventing performance degradation.

- Adaptive learning: Developing algorithms that allow the model to continuously learn and adapt to changing environmental conditions and dust characteristics can improve its accuracy and robustness over time.
- Integration with other plant systems: Integrating the dust classification system with other plant monitoring systems, such as weather forecasting and maintenance scheduling, can provide a more comprehensive view of plant operations and enable predictive maintenance.
- Cost-effective implementation: Investigating strategies to reduce the hardware and computational costs associated with deploying the system can make it more accessible for a wider range of applications, including smaller-scale solar thermal installations.

5.2 Recommendations

To train robust and accurate segmentation models based on deep learning, it is essential to establish a comprehensive and diverse proprietary database. This database should encompass a wide range of parameters, including:

- Lighting conditions: Images taken under different lighting conditions (e.g., direct sunlight, overcast, low light).
- Viewing angles: Images captured from various angles to simulate different inspection scenarios.
- Image resolution and quality: Images with varying resolutions and quality levels to account for real-world conditions.

To train effective classification models, the database may include other conditions such as defects accurately identified and labeled. This requires a meticulous process of manual or automated segmentation to delineate the boundaries of defects within the images. On the other hand, determining the optimal height for image acquisition is crucial for obtaining accurate and informative data. Factors to consider include:

- Different sizes and orientations: The height should be adjusted to ensure that the entire collector is captured in the image.
- Image resolution: A higher acquisition height may be necessary to capture sufficient detail.
- Environmental conditions: The height may need to be adjusted based on factors like wind, rain, or other environmental conditions that could affect image quality.
- Conducting experiments to evaluate the impact of different acquisition heights on image quality and defect detection accuracy, it is possible to determine the most suitable height.

References

Ahmad, P., Jin, H., Alroobaea, R., Qamar, S., Zheng, R., Alnajjar, F., and Aboudi, F. (2021). Mh unet: A multi-scale hierarchical based architecture for medical image segmentation. *IEEE Access*, 9:148384–148408. 22

AlZahrani, A. A. and Dincer, I. (2018). Energy and exergy analyses of a parabolic trough solar power plant using carbon dioxide power cycle. *Energy Conversion and Management*, 158:476–488. 9, 11

Alzubaidi, L., Zhang, J., Humaidi, A. J., Al-Dujaili, A., Duan, Y., Al-Shamma, O., Santamaría, J., Fadhel, M. A., Al-Amidie, M., and Farhan, L. (2021). Review of deep learning: concepts, cnn architectures, challenges, applications, future directions. *Journal of big Data*, 8:1–74. 14

Azouzoute, A., Merrouni, A. A., Garoum, M., et al. (2020). Soiling loss of solar glass and mirror samples in the region with arid climate. *Energy Reports*, 6:693–698. 3

Bagavathiappan, S., Lahiri, B. B., Saravanan, T., Philip, J., and Jayakumar, T. (2013). Infrared thermography for condition monitoring - a review. 3

Bertozzi, M., Broggi, A., Cellario, M., Fascioli, A., Lombardi, P., and Porta, M. (2002). Artificial vision in road vehicles. *Proceedings of the IEEE*, 90(7):1258–1271. 16

Biryukov, S., Faiman, D., and Goldfeld, A. (1999). An optical system for the quantitative study of particulate contamination on solar collector surfaces. *Solar Energy*, 66(5):371–378. 3

Bouaddi, S., Ihlal, A., and Fernández-García, A. (2015). Soiled csp solar reflectors modeling using dynamic linear models. *Solar Energy*, 122:847–863. 3

Cipriani, G., D'Amico, A., Guarino, S., Manno, D., Traverso, M., and Dio, V. D. (2020). Convolutional neural network for dust and hotspot classification in pv modules. *Energies*, 13. 3

Cohen, G., Kearney, D., and Price, H. (1999). Performance history and future costs of parabolic trough solar electric systems. *Le Journal de Physique IV*, 9(PR3):Pr3–169. 3

Dhruv, P. and Naskar, S. (2020). Image classification using convolutional neural network (cnn) and recurrent neural network (rnn): A review. *Machine learning and information processing: proceedings of ICMLIP 2019*, pages 367–381. 16

DJI (Jan 10th, 2021). `https://www.dji.com/mx/zenmuse-z3/`. 20

Erdenedavaa, P., Rosato, A., Adiyabat, A., Akisawa, A., Sibilio, S., and Ciervo, A. (2018). Model analysis of solar thermal system with the effect of dust deposition on the collectors. *Energies*, 11(7):1795. 2, 9

Foundation, The Python Software (Nov 19th, 2020). `https://www.python.org/`. 27

Frein, A. and Valenzuela, L. (2018). Solar thermal energy in industrial processes. *Energy Conversion and Management*, 156:352–364. 10

Ghazi, S., Sayigh, A., and Ip, K. (2014). Dust effect on flat surfaces–a review paper. *Renewable and Sustainable Energy Reviews*, 33:742–751. 12

Hachicha, A. A., Al-Sawafta, I., and Hamadou, D. B. (2019). Numerical and experimental investigations of dust effect on csp performance under united arab emirates weather conditions. *Renewable Energy*, 143:263–276. 3

Heimsath, A. and Nitz, P. (2019). The effect of soiling on the reflectance of solar reflector materials-model for prediction of incidence angle dependent reflectance and attenuation due to dust deposition. *Solar Energy Materials and Solar Cells*, 195:258–268. 4

Huang, X., Wang, X., Lv, W., Bai, X., Long, X., Deng, K., Dang, Q., Han, S., Liu, Q., Hu, X., et al. (2021). Pp-yolov2: A practical object detector. *arXiv preprint arXiv:2104.10419*. 17

Hussain, M., Bird, J. J., and Faria, D. R. (2018). A study on cnn transfer learning for image classification. In *UK Workshop on computational Intelligence*, pages 191–202. Springer. 26

IBM (Nov 19th, 2020). `www.ibm.com/knowledgecenter/neuralnet_model.html`. 15

Kalogirou, S. A. (2009). *Parabolic Trough Solar Collectors for Industrial Heat Applications*. Springer. 10

Kembuan, O., Rorimpandey, G. C., and Tengker, S. M. T. (2020). Convolutional neural network (cnn) for image classification of indonesia sign language using tensorflow. In *2020 2nd International Conference on Cybernetics and Intelligent System (ICORIS)*, pages 1–5. IEEE. 25

LACYQS Laboratorio Nacional de Sistemas de Concentracion y Quimica Solar (Nov 19th, 2020). `http://concentracionsolar.org.mx/`. 7

Library, Open Source Computer Vision (Nov 19th, 2020). `https://www.python.org/`. 20, 31

Los Santos-García, D., Nahmad-Molinari, Y., Nieto-Navarro, J., Alanís-Ruiz, C., Patiño-Jiménez, F., et al. (2016). Construction and testing of lightweight and low-cost pneumatically inflated solar concentrators. *International Journal of Photoenergy*, 2016. 8, 9, 10

Medsker, L. R. and Jain, L. (2001). Recurrent neural networks. *Design and Applications*, 5(64-67):2. 16

Meng, C., Sun, M., Yang, J., Qiu, M., and Gu, Y. (2017). Training deeper models by gpu memory optimization on tensorflow. In *Proc. of ML Systems Workshop in NIPS*, volume 7. 26, 27

Moghimi, M. A. and Ahmadi, G. (2018). Wind barriers optimization for minimizing collector mirror soiling in a parabolic trough collector plant. *Applied Energy*, 225:413–423. 7, 9

Pérez-Denicia, E., Fernández-Luqueño, F., Vilariño-Ayala, D., Montaño-Zetina, L. M., and Maldonado-López, L. A. (2017). Renewable energy sources for electricity generation in mexico: A review. *Renewable and Sustainable Energy Reviews*, 78:597–613. 6, 8

Pettit, R. and Freese, J. (1980). Wavelength dependent scattering caused by dust accumulation on solar mirrors. *Solar energy materials*, 3(1-2):1–20. 3

ROJO, A. R. (2017). Análisis y simulación de cargas de viento en un concentrador solar de canal parabólico mediante la aplicación de software. 10, 11

Ronneberger, O., Fischer, P., and Brox, T. (2015). U-net: Convolutional networks for biomedical image segmentation. In *International Conference on Medical image computing and computer-assisted intervention*, pages 234–241. Springer. 22

Şahin, A. D. (2007). A new formulation for solar irradiation and sunshine duration estimation. *International Journal of Energy Research*, 31(2):109–118. 12

Salari, A. and Hakkaki-Fard, A. (2019). A numerical study of dust deposition effects on photovoltaic modules and photovoltaic-thermal systems. *Renewable Energy*, 135:437–449. 2

Taqi, A. M., Awad, A., Al-Azzo, F., and Milanova, M. (2018). The impact of multi-optimizers and data augmentation on tensorflow convolutional neural network performance. In *2018 IEEE Conference on Multimedia Information Processing and Retrieval (MIPR)*, pages 140–145. IEEE. 24

TensorFLow (Jun 20th, 2021). `https://www.tensorflow.org/`. 31

Usamentiaga, R., Fernández, A., and Carús, J. L. (2020). Evaluation of dust deposition on parabolic trough collectors in the visible and infrared spectrum. *Sensors (Switzerland)*, 20:1–20. 2

Vivar, M., Herrero, R., Antón, I., Martínez-Moreno, F., Moretón, R., Sala, G., Blakers, A. W., and Smeltink, J. (2010). Effect of soiling in cpv systems. *Solar Energy*, 84(7):1327–1335. 3

Wei, X.-S., Song, Y.-Z., Mac Aodha, O., Wu, J., Peng, Y., Tang, J., Yang, J., and Belongie, S. (2021). Fine-grained image analysis with deep learning: A survey. *IEEE transactions on pattern analysis and machine intelligence*, 44(12):8927–8948. 14

Yfantis, E. and Fayed, A. (2014). A camera system for detecting dust and other deposits on solar panels. *Advances in Image and Video Processing*, 2. 13

Zefri, Y., Elkettani, A., Sebari, I., and Lamallam, S. A. (2018). Thermal infrared and visual inspection of photovoltaic installations by uav photogrammetry—application case: Morocco. *Drones*, 2:1–24. 2

Zhao, H. and Zhang, Z. (2020). Improving neural network detection accuracy of electric power bushings in infrared images by hough transform. *Sensors (Switzerland)*, 20. 2, 18